Defect and Diffusion Forum
ISSN: 1662-9507, Vol. 426, pp 43-48
doi:10.4028/p-90qste

Submitted: 2022-09-07
Revised: 2022-12-02
Accepted: 2022-12-04
Online: 2023-06-06

The Optical Properties of the Carbon Di-Vacancy-Antisite Complex in the Light of the TS Photoluminescence Center

M. Schober[1,a*], N. Jungwirth[1,b], T. Kobayashi[2,c], J.A.F. Lehmeyer[2,d], M. Krieger[2,e], H.B. Weber[2,f], and M. Bockstedte[1,g]

[1]Institute for Theoretical Physics, Johannes Kepler University Linz, Altenbergerstr. 69, A-4040 Linz, Austria

[2]Lehrstuhl für Angewandte Physik, Department Physik, Friedrich-Alexander-Universität Erlangen-Nürnberg (FAU),
Staudststr. 7, 91058 Erlangen, Germany

[a]maximilian.schober@jku.at, [b]nicolas.jungwirth@gmx.at, [c]kobayashi@prec.eng.osaka-u.ac.jp, [d]johannes.lehmeyer@fau.de, [e]michael.krieger@fau.de, [f]heiko.weber@fau.de, [g]michel.bockstedte@jku.at

Keywords: Color Center, Photophysics, Charge-State Control, Ab Initio Theory, Photoluminescence, Stark Effect

Abstract. The TS center is a promising temperature-stable photoluminescence center in 4H SiC. Here we investigate the carbon di-vacancy-antisite complex in the framework of ab initio theory as a tentative model for the TS center. We identify optical transitions of the basal complexes with the TS lines based on excitation energies, Stark shifts, and radiative characteristics. Charge-state-control of the TS center in p- and n-type Schottky contacts is demonstrated. Our experimental findings are consistent with the positively charged carbon di-vacancy-antisite complex.

Introduction

SiC hosts color centers, such as the silicon vacancy (V_{Si}), the di-vacancy ($V_{Si}V_C$), and the carbon antisite-vacancy complex ($C_{Si}V_C$) that are relevant quantum bits and single photon sources for quantum technology [1, 2, 3]. The high potential of vacancy-related centers urges to further explore this class of defects. The carbon di-vacancy-antisite complex ($V_CC_{Si}V_C$) was earlier suggested as an annealing product of the di-vacancy (via conversion of V_{Si}) [4, 5] and of $C_{Si}V_C$ (via the attachment of V_C) [5] and therefore is expected to be a relevant defect. The theoretical investigation of this center and its photo physics is a requisite for a pending identification in experiments. Indeed, the presence of carbon and silicon dangling bonds as in $C_{Si}V_C$ suggests rich photo and spin physics that has not yet been explored.

Recently, we identified a novel thermally stable TS center in photoluminescence (PL) experiments [6]. This PL center consists of a set of three lines TS1, TS2, and TS3 with a strong response to electric fields (Stark shift) and strain [8]. Its capability to emit single photons makes this center promising. Thermal annealing enhances the intensity of the PL center at temperatures at which the PL lines of $C_{Si}V_C$ and $V_{Si}V_C$ disappear, indicating that this center may be a common annealing product. In this work we combine our experimental and theoretical approaches and investigate the photophysical properties of the TS center and $V_CC_{Si}V_C$ in 4H-SiC with the aim to unravel the supposed relation between them.

Methods

Theoretical approach.

Our theoretical approach based on hybrid density functional theory (DFT) reveals the groundstate properties of the four inequivalent configurations of $V_CC_{Si}V_C$ realized in 4H-SiC using 576 atom supercells. Their dominant excitation paths and dielectric functions are evaluated within our embedded many-body (CI-CRPA) approach [7]. Based on these results, we use constrained-occupation DFT

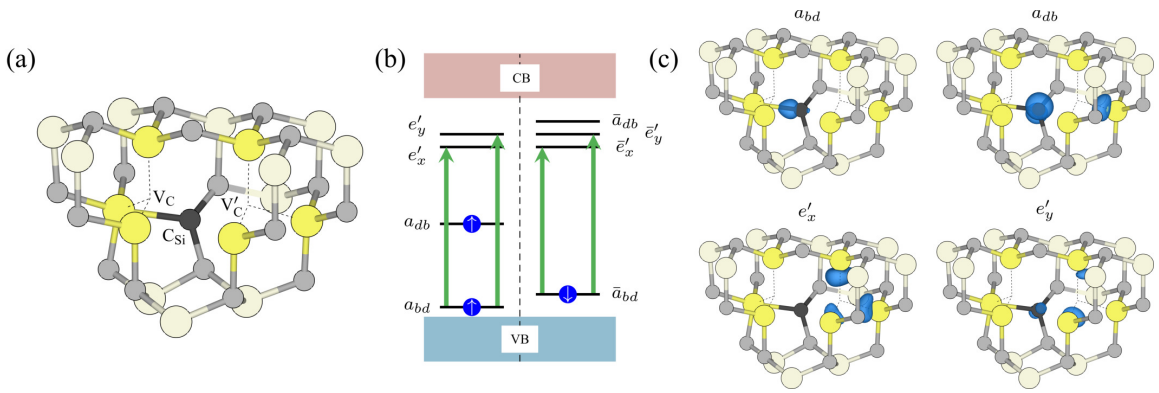

Fig. 1: Geometry and electronic structure of $V_C C_{Si} V_C{}^+$: (a) basal configuration with two carbon vacancies and the antisite at cubic and hexagonal sites (*khk*), respectively; (b) generic level scheme and occupation, where for instance the label a_{bd} ($\bar{a}_{bd}$) refers to the level with electron spin up (down) and green arrows indicate transition in the energy range of the TS lines; The indicated transitions not only occur with the depicted spin orientations but also with spin-up and spin-down interchanged. (c) defect orbitals of the basal configuration *khk*.

(CDFT) to obtain relaxed excited state geometries and Zero-Phonon Lines (ZPLs) via CI-CRPA. We classify these transitions by calculating and comparing the energy, change of static dipole moment associated with the Stark shift of the optical transitions [10, 11] and radiative characteristics with the experimental findings for the TS123 lines [6, 8].

In contrast to NV^- in diamond and the di-vacancy in 4H-SiC, $V_C C_{Si} V_C$ features a larger number of defect orbitals that couple to multi-determinant excited states in the CI-CRPA. Mapping of transitions within an effective one-electron picture (CDFT) and the many multi slater determinental representation (CI-CRPA) was done using the atomic-orbital projected single-particle reduced density matrix. This became necessary due to considerable exchange splitting in CDFT calculations and strong electron-phonon coupling in the defect states. Projections including the significant lattice sites (antisite + 6 Si-neighbors of V_C) allowed this.

Experimental approach.

In our experiments charge-state-control is implemented via Schottky contacts and doped SiC to enable carrier transport and trap filling. We use samples cut from commercial n-type and p-type 4H-SiC wafers with nominal dopant concentrations $[\mathrm{Al}] \approx 1 \cdot 10^{15}\,\mathrm{cm}^{-3}$ and $[\mathrm{N}] \approx 6 \cdot 10^{15}\,\mathrm{cm}^{-3}$, respectively. Epitaxial graphene is grown on the Si-face for electro-optical access to the color centers like in [8]. Subsequent hydrogen-intercalation converts the monolayer graphene to quasi-freestanding bilayer graphene with a higher Schottky-barrier to SiC [9]. Damage is induced by proton irradiation with a dose of $10^{15}\,\mathrm{cm}^{-2}$ and an energy of 60 keV. The generated vacancies are located in a range up to 500 nm below the surface and should mostly lie in the depletion region. Subsequent annealing at 1200°C for 30 min under Ar-atmosphere produces the TS centers. Structuring of the contacts is performed as in [8]. The measurements were performed in a home-built confocal microscope setup at a temperature of 4 K. Photoluminescence excitation was performed with a 532 nm laser.

Results

Electronic States of the Carbon Di-Vacancy-Antisite Complex

The carbon di-vacancy-antisite complex ($V_C C_{Si} V_C$) is realized in four inequivalent *axial* (hhk & kkh) and *basal* (khk & hkh) configurations, where the vacancies or the antisite occupy either hexagonal (h) or cubic (k) sites. In the axial complexes one vacancy and the antisite are oriented along the c-axis, whereas basal complexes occupy a single basal plane.

Table 1: Ionization levels of $V_CC_{Si}V_C$ relative to the valence band edge in eV. A negative U-effect occurs for $V_CC_{Si}V_C^-{}_{hkh}$, $V_CC_{Si}V_C^0{}_{khk}$, and $V_CC_{Si}V_C{}^0_{kkh}$, where the corresponding ionization levels are given in braces. These charge states are metastable. The level involving ionization by the transfer of two electrons is given next to the values in braces.

	hkh		khk		hhk		kkh	
(3+|2+)	0.54		0.50		0.52		0.51	
(2+|+)	1.31		1.25		1.25		1.28	
(+|0)	2.14		(2.78)	2.43	2.21		(2.88)	2.37
(0|-)	(3.05)	2.96	(2.09)		2.60		(1.85)	
(-|2-)	(2.87)		–		–		3.13	

As apparent from Fig. 1 (a), the antisite reconstructs towards one of the carbon vacancies V_C, forming a bond (a_{bd}) to one of the vacancy's Si atoms. Notably, this process breaks the mirror plane of basal defects, while axial configurations retain their C_{1h} symmetry. All other defect orbitals are formed from dangling bonds of the antisite (a_{db}) and the Si neighbors of the non-reconstructed vacancy V'_C. For clarity, we have labeled the latter e'_x and e'_y in analogy to the dangling bond states of $C_{Si}V_C$. Note, however, that e'_x and e'_y are not degenerate owing to the lack of symmetry. As indicated in Fig. 1 for $V_CC_{Si}V_C{}^+$, all configurations feature the same general defect level structures with some slight variations in the energetic order of axial defects and the composition of e'_x and e'_y.

The di-vacancy-antisite complex occurs in charge states ranging from $+3$ to -1. For intrinsic conditions used throughout our experiments, however, only the $+1$ state is stable. The $+2$ and the neutral complexes have a limited stability range prone to photo-ionization at typical photon energies ($h\nu > 1.3\,\text{eV}$), with the latter being even a meta-stable charge state in the khk & kkh configurations (cf. Tab. 1).

Regarding quantum applications, the spin multiplicity of the ground state is important. The $+1$ charge state posseses a spin-doublet ground state with a metastable quartett at $\approx 0.8\,\text{eV}$ (depending on the configuration). The $V_CC_{Si}V_C{}^{2+}$ on the other hand features a singlet ground state with a close lying triplet metastable state while the neutral complexes feature a triplet ground state.

Optical Properties in the Light of the TS Center

In this section we primarily focus on $V_CC_{Si}V_C{}^+$ given its dominance under intrinsic conditions. Our CI-CRPA and CDFT calculations show, that the essential optical transitions can be understood within an effective single particle picture. In Fig. 1(b), for instance, we indicate transitions paths from a_{bd} to e'_x and e'_y. Their excitation energies are given in Tab. 2 for all configurations. These energies lie in the range of the TS lines, given the systematic underestimation by $\approx 0.2\,\text{eV}$ within the CI-CRPA approach [7]. We find further transitions ($a_{db} \rightarrow e'_x$ & $a_{db} \rightarrow e'_y$) at energies below $1.1\,\text{eV}$ we do not describe in detail here. Instead we focus on the analysis of the former transitions in the context of the TS lines.

In our previous work [8], the directional-dependence of the Stark shift of TS123 has been analyzed, showing that the line shift is associated with a static dipole moment $\Delta\vec{p}$ along the next-nearest neighbor (NNN) direction . $\Delta\vec{p}$ reflects the change of the static dipole moment of the ground and excited state geometries. The orientation of $\Delta\vec{p}$ is incompatible with axial complexes, which have mirror symmetry with respect to the nearest neighbor (NN) direction. Hence, axial complexes cannot explain the TS123 lines. This symmetry is missing in the basal complexes. Our calculation of $\Delta\vec{p}$ yields orientations along the NNN direction for the $a_{bd} \rightarrow e'_x$ and $a_{bd} \rightarrow e'_y$ transitions. In contrast, $\Delta\vec{p}$ of $\bar{a}_{bd} \rightarrow \bar{e}'_x$ and $\bar{a}_{bd} \rightarrow \bar{e}'_y$ is oriented along NN, and thus incompatible with the TS center. Therefore the TS123 lines may only be explained by the four remaining transitions of the basal complexes.

Table 2: Selected transitions of $V_C C_{Si} V_C{}^+$ in eV as calculated by CI-CRPA including relaxation of the excited state within the CDFT approach. The transitions are also indicated in Fig. 1b.

transition	hkh	khk	hhk	kkh
$a_{bd} \rightarrow e'_x$	1.38	1.37	1.47	1.36
$a_{bd} \rightarrow e'_y$	1.35	1.31	1.55	1.63
$\bar{a}_{bd} \rightarrow \bar{e}'_x$	1.24	1.36	1.23	1.22
$\bar{a}_{bd} \rightarrow \bar{e}'_y$	1.34	1.28	0.96	1.36

Our calculations suggest the presence of strong electron-phonon coupling between energy surfaces of degenerate excited states. Hence, we expect that this coupling leads to the formation of vibronic states. They require treatment beyond the present approach and should explain the TS lines. Further confidence in this argument comes from the polar plots of the radiative characteristics: Here we find that the transition dipole moments are oriented along the NNN directions, as observed in the experiment. However, owing to the flat potential energy surfaces, they show orientational variations as e'_x and e'_y evolve on their surfaces.

Charge-State-Control of the TS Center

By applying a voltage at the graphene contact, we aim to change the charge-state of the TS centers inside the depletion region. Figure 2 displays the PL spectrum of the TS defect without bias voltage and as a function of the voltage applied at the graphene-SiC Schottky contact. The TS lines in p-type and n-type samples correspond to the ones observed in HPSI samples [6]. Note, however that TS2,TS3 in n-type appear with higher intensity compared to the same lines in the HPSI spectra. Moreover a peak separated from TS3 by $\Delta\lambda \sim 3\,\text{nm}$ appears at a much larger intensity than in the HPSI and p-type spectra. The origin of this peak is subject to further investigation. The PL intensity in the p-type SiC is strongly influenced by the voltage, the TS lines vanish almost completely for -40 V. For the n-type SiC only low voltages were possible because of increasing current already at lower voltages. However, a similar behavior still becomes apparent with a well visible decrease already at -5 V. Additionally, the PL signal increases when a positive voltage is applied. Note that the applied voltage causes electrical fields along the c-axis for which a visible Stark effect as reported in [8] for basal field configurations and larger voltages cannot be expected.

According to TRIM-calculations, the density of vacancies produced by the proton irradiation is about five orders of magnitude higher than the doping density. Even after annealing, it is reasonable to assume that the Fermi level is pinned in the mid-gap region in both samples. With increasing voltage the Fermi-level shifts away from the valence band edge towards the conduction band edge. The observed increasing PL-intensity implies that the underlying defect gradually changes from an inactive to the active charge state. Inspection of the ionization levels in Table 1 suggests an identification of the on-set of the decreasing PL intensity for negative voltages with the (2+|+) transition.

Summary

In conclusion, we have investigated the optical properties of the carbon di-vacancy-antisite complex in 4H-SiC in the light of the recently discovered TS center. The two basal complexes possess optical transitions with energies, Stark shifts, and radiative characteristics matching the findings for the TS lines. Using n- and p-type Schottky diodes with epitaxial graphene as transparent electrode, we demonstrate the charge-state control of the TS center in agreement with the calculated stability range of $V_C C_{Si} V_C{}^+$. Although additional work is required to clarify all spectral features of the center and our model, our findings suggest a tentative identification of the TS center with the positively charged carbon di-vacancy-antisite complex.

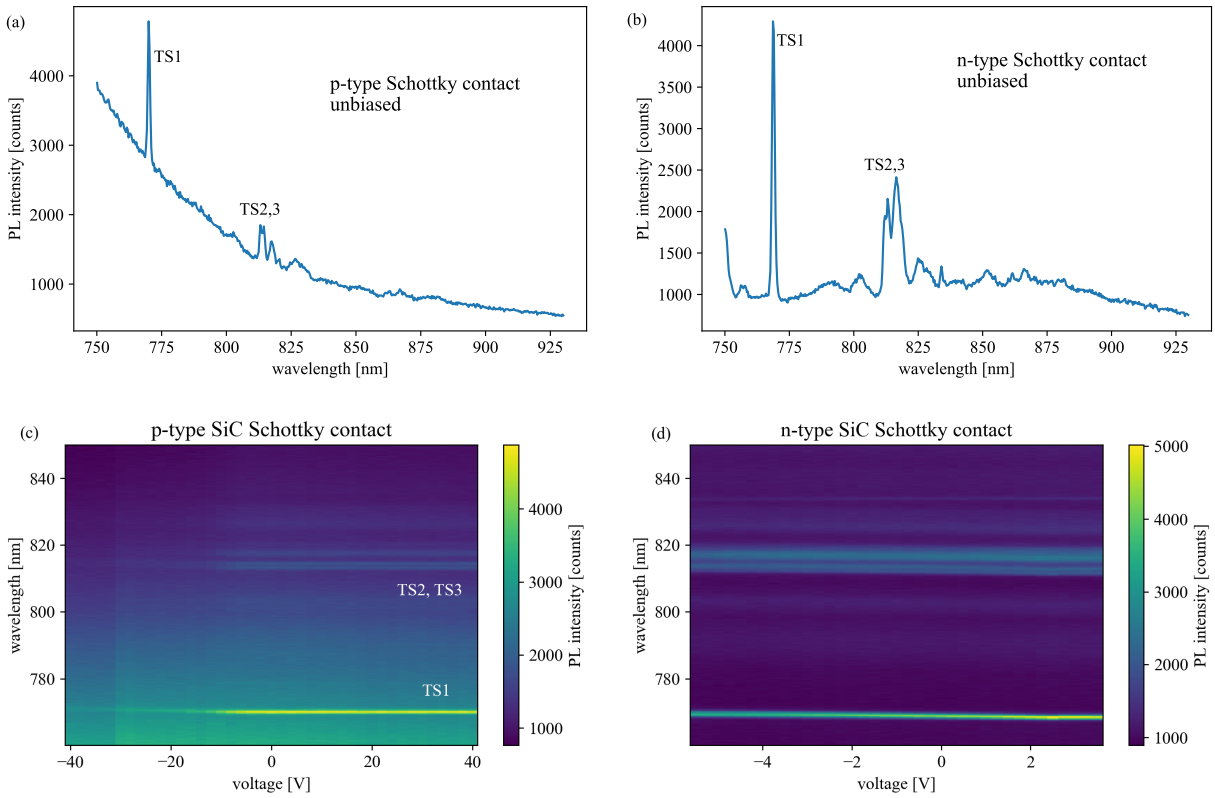

Fig. 2: Spectra of the TS-center in p-type and n-type 4H-SiC. PL-spectra of the unbiased (a) p-type and (b) n-type Schottky contacts. (c) Intensity of the TS-lines over applied voltage at the graphene contact for p-type SiC: a strong decrease in PL intensity is visible for a negative voltage at the graphene contact. The positions of the TS1, TS2 and TS3 lines are marked in the picture. All three lines display the same behavior. (d) same as (c) for n-type SiC. The lines TS1-TS3 also exhibit a slight decrease in PL-intensity for negative voltages. Additionally, the PL signal increases with a positive voltage.

Acknowledgement

We acknowledge financial support by German Research Foundation (DFG, QuCoLiMa, SFB/TRR 306, Project No. 429529648). MS and MB received financial support from the Austrian Science Fund (FWF, grant I5195). The project profited from very generous computer time provided by the Erlangen National High Performance Computing Center (NHR@FAU) of the Friedrich-Alexander-Universität Erlangen-Nürnberg (FAU) and the Vienna Scientific Cluster (VSC).

References

[1] H. Kraus, V. A. Soltamov, D. Riedel, S. Väth, F. Fuchs, A. Sperlich, P. G. Baranov, V. Dyakonov, and G. V. Astakhov, Nat. Phys. 10 (2014) 157.

[2] D. J. Christle, A. L. Falk, P. Andrich, P. V. Klimov, J. U. Hassan, N. T. Son, E. Janzén, T. Ohshima, and D. D. Awschalom, Nat. Mater. 14 (2015) 160.

[3] S. Castelletto, B. C. Johnson, V. Ivady, N. Stavrias, T. Umeda, A. Gali, T. Ohshima, Nat. Mater. 13 (2014) 151.

[4] U. Gerstmann, E. Rauls, H. Overhof, Phys. Rev. B 70 (2004) 201204(R).

[5] E. M. Y. Lee, A. Yu, J. J. de Pablo, G. Galli, Nat. Commun. 12 (2021) 63.

[6] M. Rühl, C. Ott, S. Götzinger, M. Krieger and H.B. Weber, Appl. Phys. Lett. 113 (2018) 122102.

[7] M. Bockstedte, F. Schütz, T. Garratt, V. Ivády and A. Gali, npj Quant Mater 3 (2018) 31.

[8] M. Rühl, J. Lehmeyer, R. Nagy, M. Weisser, M. Bockstedte, M. Krieger and H.B. Weber, New J. Phys. 23 (2021) 073002.

[9] S. Hertel, D. Waldmann, J. Jobst, A. Albert, M. Albrecht, S. Reshanov, A. Schöner, M. Krieger and H.B. Weber, Nat. Commun. 3 (2012) 957.

[10] R.D. King-Smith and D. Vanderbilt, Phys. Rev. B 47 (1993) 1651(R).

[11] P. Udvarhelyi, R. Nagy, F. Kaiser, S.-Y. Lee, J. Wrachtrup, and A. Gali, Phys. Rev. Applied 11 (2019) 044022.

[12] J. A. F. Lehmeyer, A. Fuchs, M. A. Popp, M. Krieger, H.B. Weber, Strain dependent photoluminescence line shifts of the TS color center in 4H-SiC, Material Science Forum, Conference Proceedings ICSCRM 2022.